

We are IntechOpen, the world's leading publisher of Open Access books Built by scientists, for scientists

6,900

Open access books available

186,000

International authors and editors

200M

Downloads

Our authors are among the

154

Countries delivered to

TOP 1%

most cited scientists

12.2%

Contributors from top 500 universities



WEB OF SCIENCE™

Selection of our books indexed in the Book Citation Index
in Web of Science™ Core Collection (BKCI)

Interested in publishing with us?
Contact book.department@intechopen.com

Numbers displayed above are based on latest data collected.
For more information visit www.intechopen.com



Impedance Spectroscopy: A Powerful Technique for Study of Electronic Ceramics

*Shukdev Pandey, Devendra Kumar, Om Parkash
and Lakshman Pandey*

Abstract

Electronic ceramics are technological materials having a vast variety of applications such as actuators and sensors, computer memories, electrically controlled microwave tuning devices for RADAR, etc. and are playing key role in electronics industry today. An electronic ceramic component can be visualised as grain-grain boundary-electrode system. Impedance spectroscopy is being widely used to separate out contributions of these to the overall property of a ceramic. This involves equivalent circuit models. To facilitate development of suitable equivalent circuit models and obtain values of the components, some most useful circuits with their simulated behaviour are presented. Steps highly useful in the modelling process are summarised. The procedure of impedance spectroscopy is illustrated by analysing the impedance data of the ceramic system $\text{BaFe}_x\text{Ti}_{1-x}\text{O}_3$ ($x = 0.05$) containing two phases.

Keywords: electronic ceramics, impedance spectroscopy, equivalent circuit models, CPE, CNLS, grain-boundaries, ceramic-electrode interface

1. Introduction

Ceramics are inorganic non-metallic solids that have been processed and shaped by heating at high temperatures. Modern ceramics include oxides, nitrides, carbides, etc. and constitute a large fraction of technologically useful materials at present. Ceramics, whose electrical, magnetic, or optical properties are used in devices are broadly termed as electro-ceramics and are being heavily used as electrical insulators, TV baluns, mobile antennas and speakers, substrates for electronic circuits, computer memories, magnetic recording heads, high-temperature heating elements, cryogenic sensors, microwave tuning devices for RADAR applications, etc. [1–3]. The as-prepared ceramics are usually in powder form that are processed and shaped for device applications by subjecting to suitable sintering procedure. A ceramic piece thus consists of small crystallites called grains that are joined together in random orientations. The joining region called the grain boundary has, due to mismatch, strained bonds. Properties of grain boundary, therefore, are different from those of grains and highly depend upon the processing variables such as heating/cooling rates, presence of external fields, atmosphere, etc. By changing these variables and starting ingredients, behaviour of grains and grain boundary

may be altered. It is the interplay between the grain and grain boundary behaviour that bestows ceramics with some very useful properties. Ceramics prepared by controlled crystallisation of glass are called glass-ceramics where the grain boundary consists of the uncrystallised glass [1, 4, 5]. The understanding and controlling of this interplay with the help of processing variables, additives, ingredients, reduction in grain size dwelling in nanometre range or compositing, with a view to develop desired, unforeseen and technologically useful properties, is the subject of intensive research activities at present. For device applications, a ceramic piece is usually connected to some other system through electrodes. Thus, an electronic component may be treated as grain-grain boundary-electrode system where the overall observed properties would have contributions from all these [1]. In order to develop ceramics having desired and reproducible properties, these individual contributions must be separated out. For this, impedance spectroscopy is a very useful technique [6]. It not only helps in developing the understanding of the processes but also provides with an equivalent circuit model for the system that may be used for simulation purposes [1, 6]. Impedance spectroscopic studies proceed with the measurement of electrical impedance as function of frequency and interpretation of the data by using suitable equivalent circuit model that seems appropriate to represent various charge transfer processes in the system. The values of the components used in the model are then obtained by using a least-squares procedure to fit the experimental impedance data with that simulated by using the chosen model. The choice of the most suitable model is a difficult process. Even if a model has been conceived, estimating the values of the components of the model, so much required for the least-squares programs, is not always straightforward. This poses some inconvenience to the worker. Developing a suitable model and obtaining these estimates are greatly facilitated by comparing the experimental plots with those simulated for various models and considering different charge transfer processes thought to be possibly present in the system. In what follows, basics of impedance spectroscopy and some very useful models with their simulated behaviour are presented. Analysis of impedance spectroscopic data on ceramic system $\text{BaFe}_x\text{Ti}_{1-x}\text{O}_3$ ($x = 0.05$) containing two phases is also presented as illustration. The focus is how to choose a model and how to get an estimate of the values of the components used in the model.

2. Basics of impedance spectroscopy

Impedance spectroscopy essentially involves measurement of real and imaginary parts of electrical impedance ($Z^* = Z' - j Z''$, $j = \sqrt{-1}$) of a system as function of frequency ($\omega = 2\pi f$) for various parameters of interest such as composition, temperature, etc. The values of Z' and Z'' are plotted as function of frequency (Z' , Z'' vs. $\log f$) and also in complex plane (i.e. Z'' vs. Z'). These complex plane plots are usually distorted semicircular overlapping arcs. By looking at the shapes of these plots, charge transfer processes present in the system and accessible in the measurement frequency range are inferred. This is greatly facilitated by comparing the experimental plots with those simulated for possible equivalent circuit models for the system. Detailed discussion on impedance spectroscopy and equivalent circuit models has been presented by Barsoukov and Macdonald [6], Jonscher [7], and Pandey et al. [8]. Due to ready availability of versatile impedance analysers working in extended frequency ranges and ease of measurements, impedance spectroscopy has emerged as a very popular and powerful tool in recent years and is being widely used in various fields encompassing materials technology, electrochemistry,

biology, medical diagnostics, agriculture, dairy and fruit production ([9] and references therein).

The electrical behaviour of a system can be expressed in terms of interrelated functions known as impedance ($Z^* = Z' - j Z''$), admittance ($Y^* = (Z^*)^{-1} = Y' + j Y''$), permittivity ($\epsilon^* = (j \omega C_0 Z^*)^{-1} = \epsilon' - j \epsilon''$), and modulus ($M^* = (\epsilon^*)^{-1} = j \omega C_0 Z^* = M' + j M''$), C_0 being the capacitance of the empty cell used to house the sample. These are broadly termed as immittance functions and are conveniently used to develop equivalent circuit models for the sample-electrode system [6, 8, 9]. A charge transfer process would have a certain time constant and would respond in the corresponding frequency region. A parallel RC circuit (**Figure 1(a)**) possesses one time constant RC and is thus conveniently used to represent one charge-transfer process. The impedance of this model circuit is given as

$$Z' = \frac{R}{1 + (\omega CR)^2}, Z'' = \frac{\omega CR^2}{1 + (\omega CR)^2} \tag{1}$$

Z' and Z'' satisfy the relation

$$\left(Z' - \frac{R}{2}\right)^2 + Z''^2 = \left(\frac{R}{2}\right)^2 \tag{2}$$

which is equation of a circle having centre at point $(R/2, 0)$, radius equal to $R/2$, intercept with Z' axis at the point $(R, 0)$, and passing through origin in Z'' vs. Z' plot. As the values of R and C are positive, the Z'' vs. Z' plot will be a semicircle (**Figure 1(b)**). On this semicircle, the peak point occurs at $Z' = R/2$. At this point, Z'' is equal to $R/2$ and $\omega CR = 1$. Also, $Z' = R$ at $\omega = 0$. Thus, if values Z' and Z'' for a sample are experimentally measured in certain frequency range and Z'' vs. Z' plot is found to be a clear semicircular arc, then a parallel RC circuit model may be used to represent the electrical behaviour of the sample, to begin with (for more details see Section 3.1). The value of intercept of the extrapolated arc with the Z' axis towards

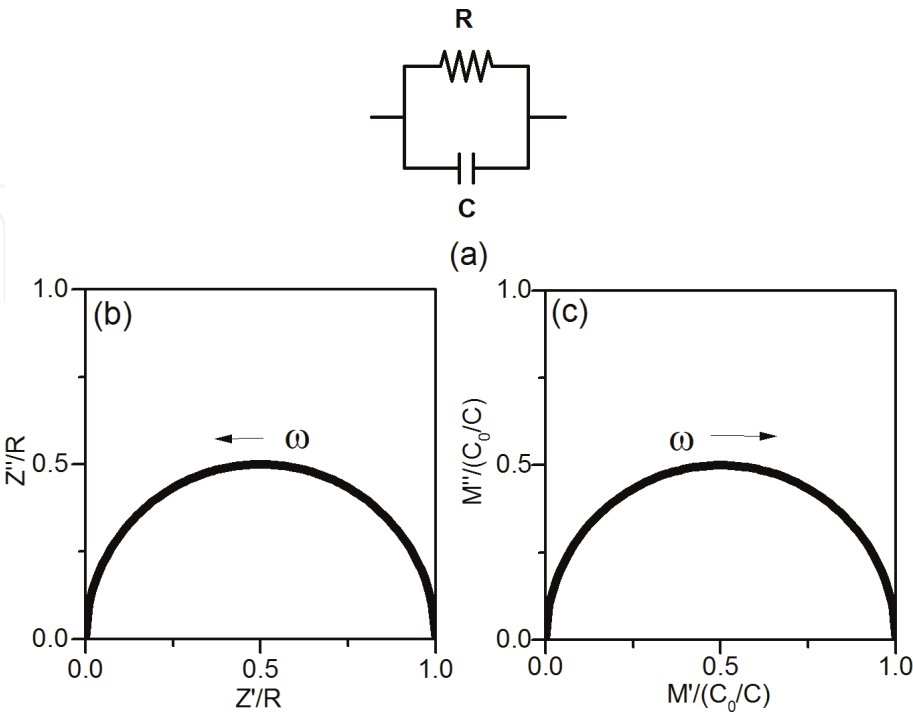


Figure 1.
(a) Equivalent circuit model containing parallel combination of R and C . Normalized (b) Z''/R vs Z'/R and (c) $M''/(C_0/C)$ vs $M'/(C_0/C)$ plots.

low-frequency side will give the value of R. The value of C can be obtained by noting the frequency where the arc peaks and using the relation $\omega CR = 1$.

For this model, M' and M'' are given as

$$M' = \omega C_0 \left(\frac{\omega CR^2}{1 + \omega^2 C^2 R^2} \right), M'' = \omega C_0 \left(\frac{R}{1 + \omega^2 C^2 R^2} \right) \quad (3)$$

which satisfy the relation

$$\left(M' - \frac{C_0}{2C} \right)^2 + M''^2 = \left(\frac{C_0}{2C} \right)^2 \quad (4)$$

Eq. (4) indicates that M'' vs. M' plot would be a semicircular arc passing through the origin and having intercept at $M' = C_0/C$ and centre at $(C_0/2C, 0)$ (**Figure 1(c)**). On this plot, M'' would peak at frequency where $\omega CR = 1$. Value of M' becomes equal to C_0/C as $\omega \rightarrow \infty$. Thus, by using M'' vs. M' plot of the same experimental data, C can be obtained by noting the high-frequency intercept in the M'' vs. M' plot. The value of R can be obtained by using this value of C and noting the frequency where M'' peaks. In the M'' vs. M' plot, the arc traverses from left to right whereas in Z'' vs. Z' plot, it traverses from right to left as the frequency is increased.

Choice of a model to represent a system is a difficult process, becoming more so since same behaviour can be simulated by different models [6]. The choice is greatly facilitated by comparing the experimental plots with those simulated for various models and considering the processes that might be present in the system with a preference to simple models to start with. When the complex plane plots display more than one arcs, presence of more polarisation/charge transfer processes is inferred. A general practice is to consider one RC circuit to represent one process and connect more RCs in series to develop an equivalent circuit model. Thus for representing grain-grain boundary-electrode system in a ceramic, a model comprising three parallel RCs connected in series might be taken [1]. It has been found that usually combinations of resistances (R) and capacitances (C) suffice for dielectrics, combinations of R and inductance L suffice for magnetic systems, and combinations of R, L and C suffice for ferro-/piezoelectrics [6–8, 10–20]. Sometimes, it is found that the lumped-component type of models do not yield good fits and their simulated patterns do not show even qualitative resemblance with the experimental plots. In those cases, attempt is made to represent the data by models involving constant phase angle elements (CPE) [6, 9] that are considered to correspond to some sort of distribution in the material properties. The values of the components used in the model are estimated by comparing the experimental plots with the simulated ones. These values are obtained more accurately by fitting the experimental data with complex non-linear least-square (CNLS) procedure using these values as initial guesses. For cases, where it is not possible to decide upon an appropriate model, equivalent circuits models that seem to be most probable to represent the processes thought to be possibly present, or to be dormant but becoming dominant as some variables change, in the system may be considered and the model that yields the lowest value of sum of squares of errors in the CNLS runs may be accepted [6].

In order to facilitate a prompt development of an equivalent circuit model for electronic ceramics, some very important clues have been given in [9] and are summarised below for a ready reference.

1. The experimental data can be represented in any of the formalisms (Z, M, Y and ϵ) and interpreted. However, analysis by using only one formalism might lead to erroneous conclusions and two or more functions such as Z and M should be used [6, 8].

2. If plots of both Z'' vs. Z' and M'' vs. M' are clear semicircles passing through origin, then the system may be represented by a model having one parallel RC and presence of one process may be inferred [6, 8].
3. Appearance of a shift towards right in M'' vs. M' plot (here, the arc traverses from left low-frequency side to right high-frequency side) and steeply rising branch at low-frequency side in the Z'' vs. Z' plot (here, the arc traverses from right to left) indicates the presence of series capacitance C in the equivalent circuit [17].
4. Appearance of a shift towards right in Z'' vs. Z' plot and steeply rising branch at high-frequency side in M'' vs. M' plot indicates the presence of series resistance R in the equivalent circuit [8, 12].
5. Appearance of two clear semicircular arcs in Z'' vs. Z' plot or M'' vs. M' plot indicates presence of two processes and equivalent circuit would contain two parallel RC's (R_1C_1 and R_2C_2). A depressed looking semicircular arc in the Z or M plots would indicate the presence of at least two processes having ratio of time constants R_2C_2/R_1C_1 in the range 1–5 [8].
6. If the experimental Z'' vs. Z' plot shows a semicircular arc with changed sign of Z'' in the whole frequency range (i.e. arc appears in fourth quadrant traversing from left to right), then a model with parallel R-L circuit may be used [11].
7. A cross over from positive values of Z'' to negative values or vice versa within the overall frequency range covered in the experiment indicates a situation of resonance and inclusion of R , C and L in the model would be needed [6, 14, 16].
8. Presence of a linear portion in the immittance plots would indicate the presence of series CPE in the model. Depressed looking immittance plots indicate that CPE connected in parallel may be included in the model [6, 9, 12, 21].

Detailed analysis of various models involving CPE is available in [6, 9]. It is believed that CPE represents distribution in properties. Therefore, when the data is well represented by a model involving CPE, presence of distribution in certain properties of ceramics is inferred. It may be mentioned that capacitor C and inductor L are used to represent the storage of electrical and magnetic forms of energy in a system. At frequencies much below resonance, the situation may be approximately modelled by considering RC's only. Similarly, a mechanically vibrating system can be analogously represented by an RLC circuit. Therefore, equivalent circuits having combinations of R , L and C may be used [14, 16] for piezoelectric ceramics. In what follows, some model circuits found very useful in study of ceramics are briefly presented. Emphasis is given to Z'' vs. Z' and M'' vs. M' plots as these were found more informative.

3. Equivalent circuit models

3.1 Model 1: parallel combinations R_1C_1 and R_2C_2 connected in series

Parallel combinations R_1C_1 and R_2C_2 connected in series [8] are shown in **Figure 2(a)** and the values for Z' and Z'' are given in Eq.(5):

$$Z' = \frac{R_1}{1 + (\omega C_1 R_1)^2} + \frac{R_2}{1 + (\omega C_2 R_2)^2}, Z'' = \frac{\omega C_1 R_1^2}{1 + (\omega C_1 R_1)^2} + \frac{\omega C_2 R_2^2}{1 + (\omega C_2 R_2)^2} \quad (5)$$

Complex plane plots for various immittance functions are shown in **Figure 2(b-e)** for $R_2/R_1 = 1$. It is seen that when the values of time constants are widely separated ($R_2 C_2/R_1 C_1 = 100$), two clear arcs appear indicating the presence of two processes. For $R_2 C_2/R_1 C_1 > 1$ but below 5, a depressed looking arc appears and when $R_2 C_2/R_1 C_1 = 1$, a single arc appears (**Figure 2(b)**).

Now let us look at the plots of **Figure 3(b-e)** for $R_2/R_1 = 100$. Here, Z'' vs. Z' plot obtained for different ratios of time constants looks like a single semicircular arc indicating presence of one process. However, the corresponding M'' vs. M' (**Figure 3(c)**) has two clear arcs indicating the presence of two processes. This indicates that inference derived from only one formalism might lead to wrong conclusions, and plots using more formalisms should be looked at together.

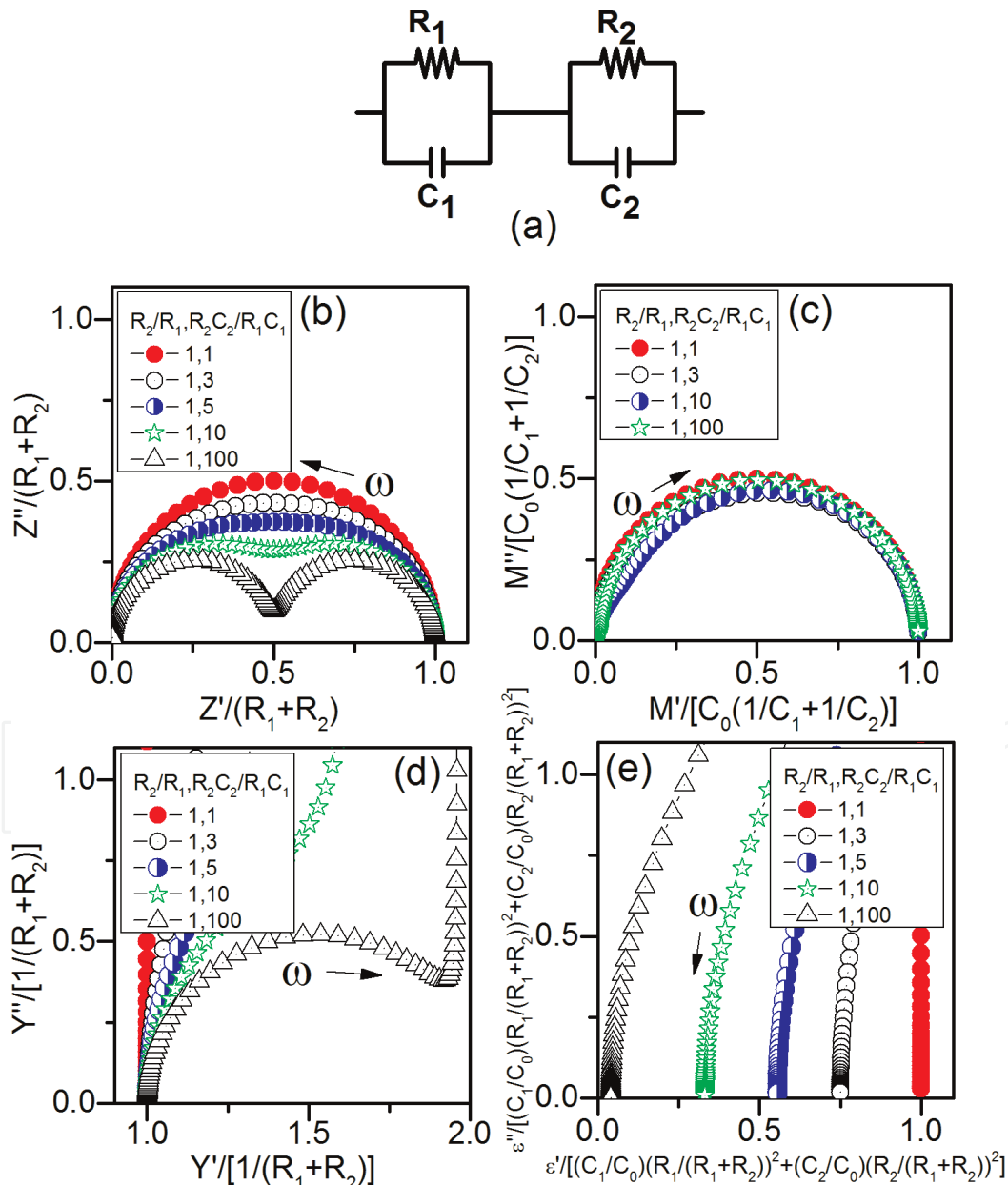


Figure 2.

(a) Equivalent circuit model containing series combination parallel $R_1 C_1$ and $R_2 C_2$. Normalized (b) $Z''/(R_1 + R_2)$ vs $Z'/(R_1 + R_2)$, (c) $M''/[C_0(1/C_1 + 1/C_2)]$ vs $M'/[C_0(1/C_1 + 1/C_2)]$, (d) $Y''/[1/(R_1 + R_2)]$ vs $Y'/[1/(R_1 + R_2)]$ and (e) $\epsilon''/[(C_1/C_0)(R_1/(R_1 + R_2))^2 + (C_2/C_0)(R_2/(R_1 + R_2))^2]$ vs $\epsilon'/[(C_1/C_0)(R_1/(R_1 + R_2))^2 + (C_2/C_0)(R_2/(R_1 + R_2))^2]$ for $R_2/R_1 = 1$ and $R_2 C_2/R_1 C_1$.

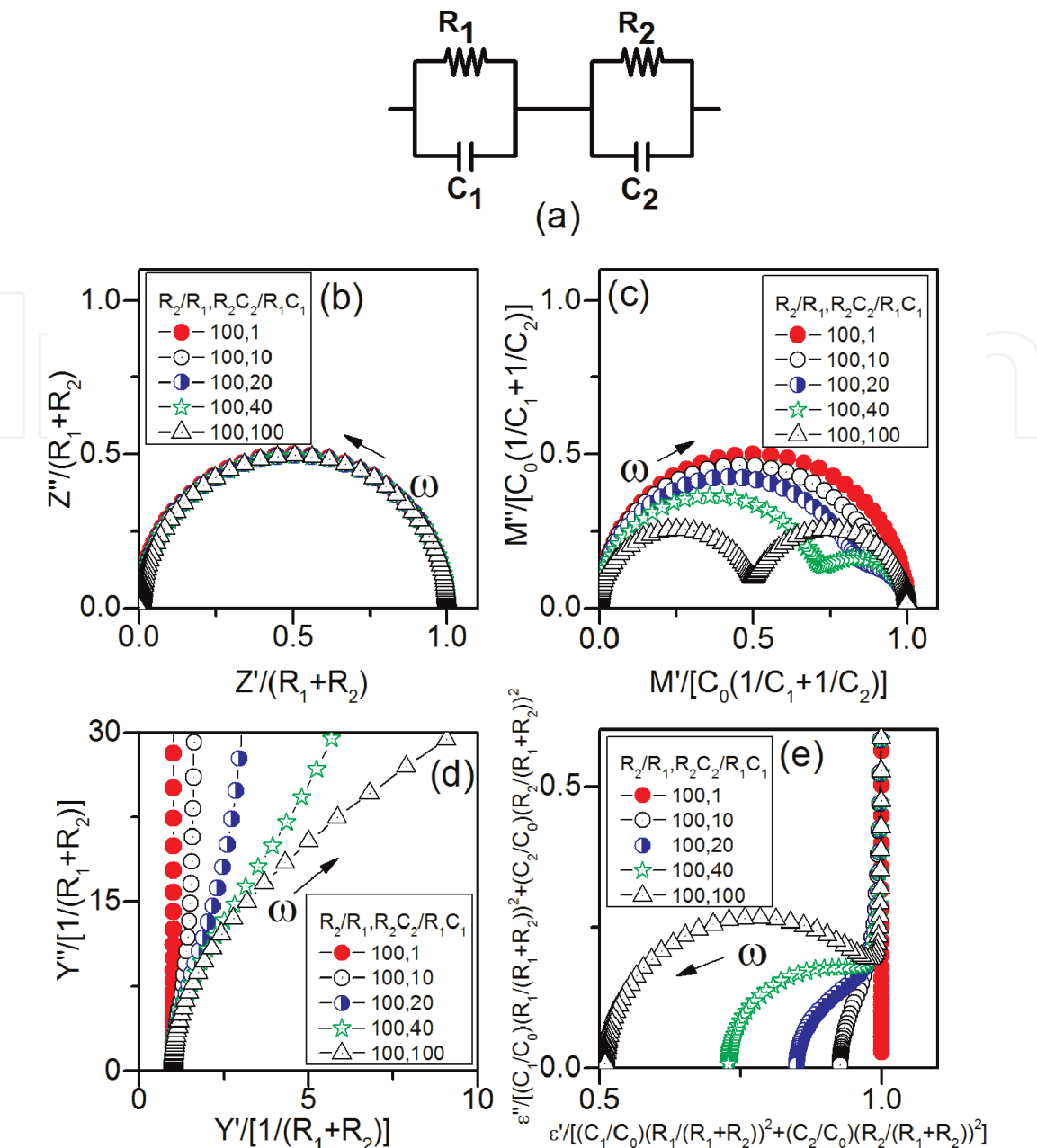


Figure 3. (a) Equivalent circuit model containing series combination of parallel R_1C_1 and R_2C_2 . Normalized (b) $Z''/(R_1 + R_2)$ vs $Z'/(R_1 + R_2)$, (c) $M''/[C_0(1/C_1 + 1/C_2)]$ vs $M'/[C_0(1/C_1 + 1/C_2)]$, (d) $Y''/[1/(R_1 + R_2)]$ vs $Y'/[1/(R_1 + R_2)]$ and (e) $\epsilon''/[(C_1/C_0)(R_1/(R_1 + R_2))^2 + (C_2/C_0)(R_2/(R_1 + R_2))^2]$ vs $\epsilon'/[(C_1/C_0)(R_1/(R_1 + R_2))^2 + (C_2/C_0)(R_2/(R_1 + R_2))^2]$ for $R_2/R_1 = 100$ and different values of R_2C_2/R_1C_1 .

3.2 Model 2: parallel combinations R_1C_1 connected in series with R_2

The model is schematically shown in **Figure 4(a)**. The values of Z' and Z'' are given as

$$Z' = \frac{R_1}{1 + (\omega C_1 R_1)^2} + R_2 \quad , \quad Z'' = \frac{\omega C_1 R_1^2}{1 + (\omega C_1 R_1)^2} \tag{6}$$

The immittance plots for this model are shown in **Figure 4(b-e)** for various values of R_2/R_1 . It is seen that Z'' vs. Z' plot (**Figure 4(b)**) shows a shift towards right, and the corresponding M'' vs. M' plot (**Figure 4(c)**) has steeply rising branch at high-frequency side.

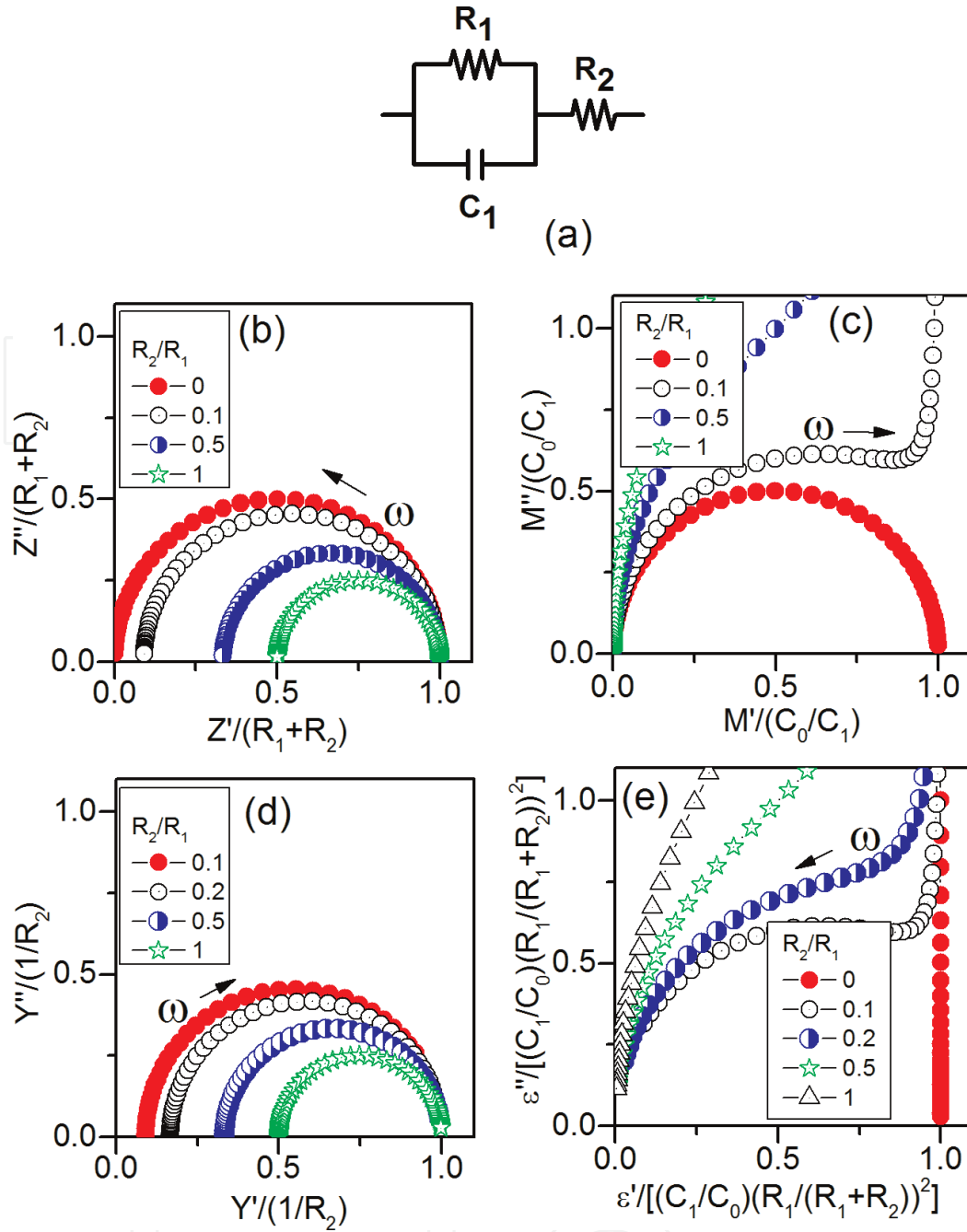


Figure 4. (a) Equivalent circuit model containing series combination of parallel R_1C_1 and R_2 . Normalized (b) $Z''/(R_1 + R_2)$ vs $Z'/(R_1 + R_2)$, (c) $M''/(C_0/C_1)$ vs $M'/(C_0/C_1)$, (d) $Y''/(1/R_2)$ vs $Y'/(1/R_2)$ and (e) $\epsilon''/[(C_1/C_0)(R_1/(R_1 + R_2))^2]$ vs $\epsilon'/[(C_1/C_0)(R_1/(R_1 + R_2))^2]$ for R_2/R_1 .

3.3 Model 3: parallel combinations R_1C_1 connected in series with C_2

Parallel combinations R_1C_1 connected in series with C_2 is shown in **Figure 5(a)**. The values of Z' and Z'' are given as [17]

$$Z' = \frac{R_1}{1 + (\omega C_1 R_1)^2}, \quad Z'' = \frac{\omega C_1 R_1^2}{1 + (\omega C_1 R_1)^2} + \frac{1}{\omega C_2} \quad (7)$$

The immittance plots for this model are shown in **Figure 5(b-e)**. It is found that Z'' vs. Z' has a low-frequency rising branch where as a shift is seen in M'' vs. M' plot.

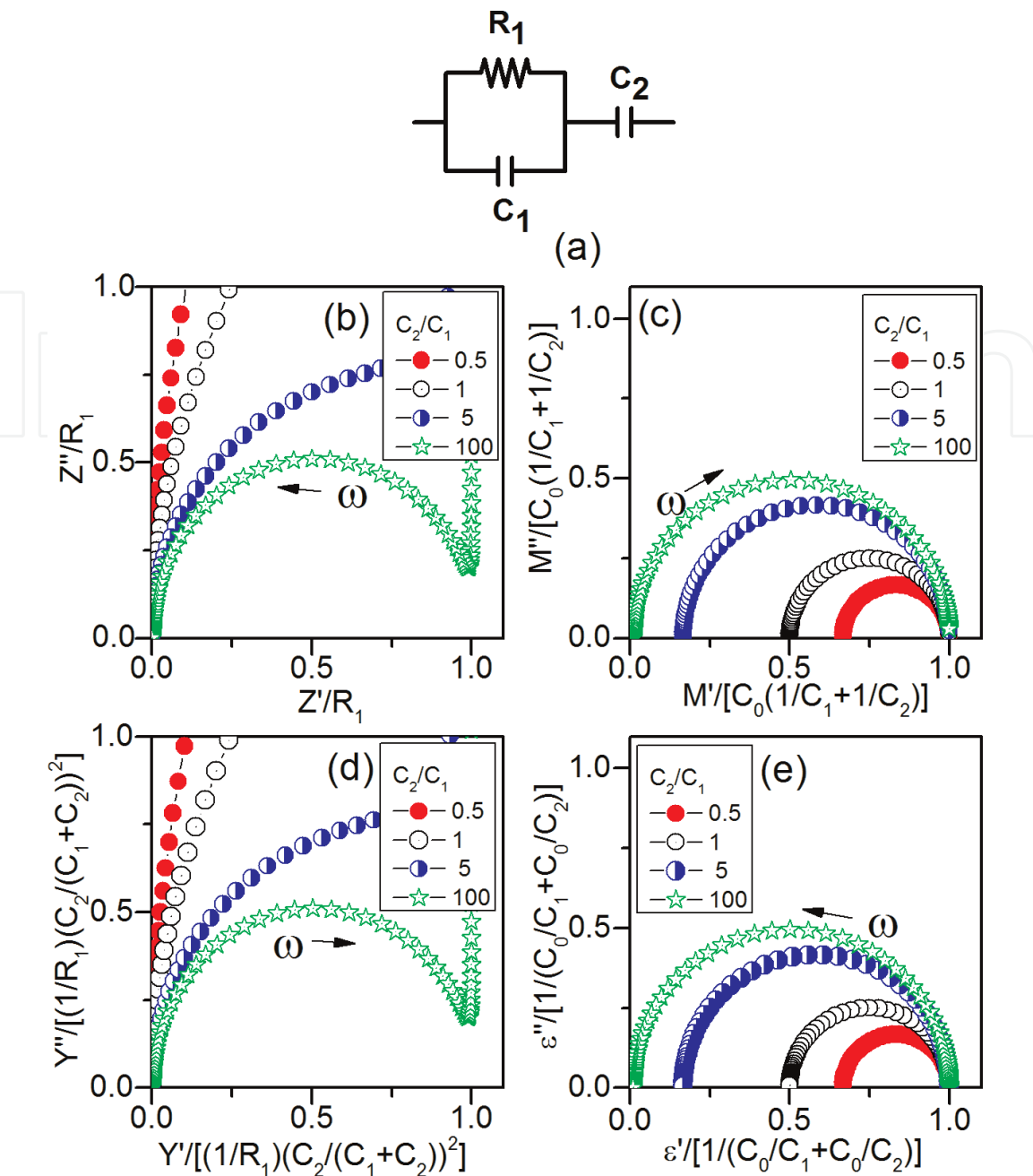


Figure 5. (a) Equivalent circuit model containing series combination of parallel R_1C_1 and C_2 . Normalized (b) Z''/R_1 vs Z'/R_1 , (c) $M''/[C_0(1/C_1 + 1/C_2)]$ vs $M'/[C_0(1/C_1 + 1/C_2)]$, (d) $Y''/[(1/R_1)(C_2/(C_1 + C_2))^2]$ vs $Y'/[(1/R_1)(C_2/(C_1 + C_2))^2]$ and (e) $\epsilon''/[1/(C_0/C_1 + C_0/C_2)]$ vs $\epsilon'/[1/(C_0/C_1 + C_0/C_2)]$ for $C_2/C_1 = 0.5, 1, 5$ and 100 .

3.4 Model 4: parallel combinations R_1C_1 , R_2C_2 connected in series with CPE

Parallel combinations R_1C_1 , R_2C_2 connected in series with a constant phase angle element (CPE) are shown in **Figure 6(a)**. The impedance of CPE is given as

$$Z_{\text{CPE}} = (Y_{\text{CPE}})^{-1} = [A_0(j\omega)^\psi]^{-1} = \frac{1}{A_0\omega^\psi} \cos\left(\frac{\psi\pi}{2}\right) - j \frac{1}{A_0\omega^\psi} \sin\left(\frac{\psi\pi}{2}\right) \quad (8)$$

Plot of imaginary part vs. real part of Z_{CPE} is a straight line with slope $\tan(\psi\pi/2)$, which remains constant as ω varies (hence the name CPE). For $\psi = 1$, the real part becomes zero and $Z_{\text{CPE}} = 1/(j\omega A_0)$ and the CPE behaves like an ideal capacitor having capacitance A_0 . For $\psi = 0$, the imaginary part becomes zero and $Z_{\text{CPE}} = 1/A_0$

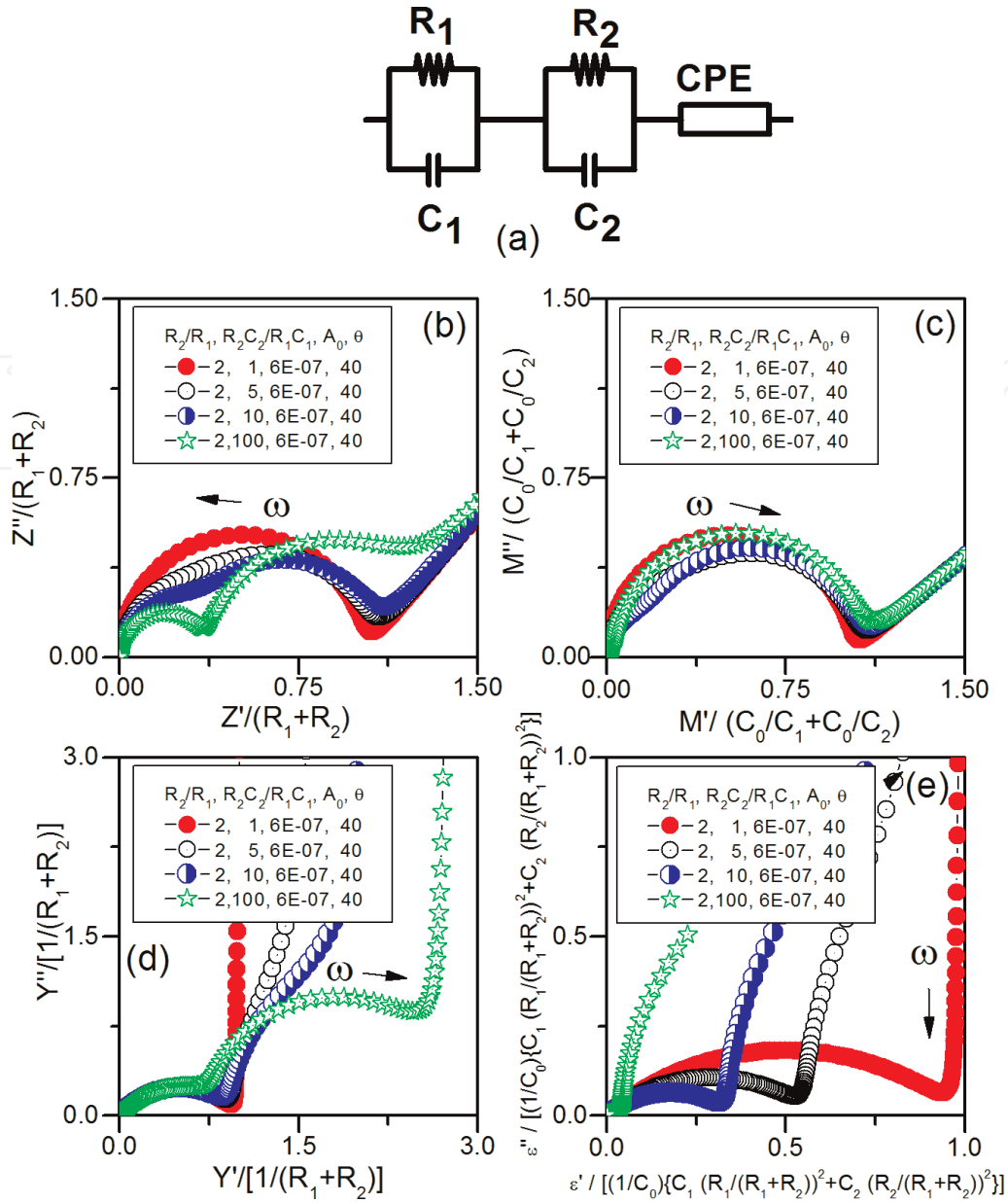


Figure 6.

(a) Equivalent circuit model containing series combination of parallel R_1C_1 , parallel R_2C_2 and CPE. Normalized (b) $Z''/(R_1 + R_2)$ vs $Z'/(R_1 + R_2)$, (c) $M''/(C_0/C_1 + C_0/C_2)$ vs $M'/(C_0/C_1 + C_0/C_2)$, (d) $Y''/[1/(R_1 + R_2)]$ vs $Y'/[1/(R_1 + R_2)]$ and (e) $\varepsilon''/[1/C_0\{C_1(R_1/(R_1 + R_2))^2 + C_2(R_2/(R_1 + R_2))^2\}]$ vs $\varepsilon'/[1/C_0\{C_1(R_1/(R_1 + R_2))^2 + C_2(R_2/(R_1 + R_2))^2\}]$ for $R_2/R_1 = 2, 5, 10, 100$, $A_0 = 6 \times 10^{-7}$ and $\theta = 40$.

and the CPE behaves like an ideal register of value $1/A_0$ [6]. The values of Z' and Z'' for the model shown in **Figure 6(a)** are given as [9, 21].

$$Z' = \frac{R_1}{1 + (\omega C_1 R_1)^2} + \frac{R_2}{1 + (\omega C_2 R_2)^2} + \left(\frac{1}{A_0 \omega^\psi} \right) \cos \left(\frac{\psi \pi}{2} \right) \quad (9)$$

$$Z'' = \frac{\omega C_1 R_1}{1 + (\omega C_1 R_1)^2} + \frac{\omega C_2 R_2}{1 + (\omega C_2 R_2)^2} + \left(\frac{1}{A_0 \omega^\psi} \right) \sin \left(\frac{\psi \pi}{2} \right) \quad (10)$$

A model comprising series combination of parallel R_1 -CPE₁ and parallel R_2 -CPE₂ is one of the models very widely used to represent the behaviour of a ceramic when the impedance plots have two depressed arcs. The reader is referred to [9] where this has been discussed by the authors in detail.

4. Experimental setup, measurements and results

Development of equivalent circuit model for representing the ceramic system $\text{BaFe}_x\text{Ti}_{1-x}\text{O}_3$ ($x = 0.05$), prepared in our laboratory, is now described as an illustration. Sample was prepared by solid state synthesis method by taking BaCO_3 (Merck 99.5%), Fe_2O_3 (Merck 99.5%) and TiO_2 (Merck 99.5%) in appropriate amounts, mixing in acetone medium for 6 hours and calcining at 1100°C for 6 hours. The calcined powder was mixed with small amount of PVA binder and pressed into disc-like (dia 12 mm, thickness 1.5 mm) pellets using uniaxial hydraulic press with 60 kN pressure. These pellets were sintered in an electrical furnace (Lenton, made in Germany) where, first, binder was removed by raising the temperature to 500°C and holding for 2 hours and then increasing the temperature to 1250°C at $5^\circ\text{C}/\text{min}$ and maintaining there for 10 hours followed by cooling it to room temperature. X-ray diffraction analysis revealed that the sample contained tetragonal and hexagonal phases in equal amounts. Impedance measurements were carried out as function of frequency (20 Hz to 1 MHz) at temperatures from 300 to 650 K. For this, the pellets were polished using emery papers of grade 1/0 and 2/0 and electroded on both sides using silver paste and cured at 600°C for 15 minutes.

The sample holder used to house the sample is schematically shown in **Figure 7(a)**. The spectroscopic and complex plane plots for M' and M'' are shown in **Figure 7(b,c)**. The corresponding Z plots are not shown for brevity. The way an equivalent circuit model representing the data was developed is now described. A quick look at the M'' vs. M' plot shown in **Figure 7(b)** reveals that there is no shift in the graph as well as no steeply rising high-frequency branch. Similar behaviour was seen in the Z plots also. Therefore, following the tips presented in Section 2, presence of series resistance or capacitance is ruled out. The plot is not a clear semicircular arc but is slightly depressed indicating the presence of more than one charge transfer processes in the system. As the sample contains two phases, we have a system comprising two types of grains, grain boundary and contact electrode interface. Therefore, an equivalent circuit model comprising four parallel RC's connected in series, where two RC's say R_1C_1 and R_2C_2 represent the two phases, R_3C_3 represents the grain boundary and R_4C_4 correspond to the sample-electrode interface, seems to be a plausible model. If we assume that $R_1C_1 < R_2C_2 < R_3C_3 < R_4C_4$ then, since electrode responses appear at low frequencies [1], R_1C_1 and R_2C_2 may be assigned to grains, R_3C_3 to grain boundary and R_4C_4 to electrode interface. The individual contributions from these RC's may be depicted by drawing tentative arcs (as shown by dotted lines in **Figure 7(b)**) making intercepts on the M' axis at C_0/C_4 , $C_0/C_4 + C_0/C_3$, $C_0/C_4 + C_0/C_3 + C_0/C_2$ and $C_0/C_4 + C_0/C_3 + C_0/C_2 + C_0/C_1$. As the plot is very symmetric, the intercepts and hence C's may be taken to be equal. By noting the values of intercepts from the graph, taking the value of C_0 as 0.6832×10^{-12} , noting the frequencies where the tentative arcs would peak and using the relation $\omega RC = 1$, the values of R' and C's are estimated as $R_1 = 362 \Omega$, $R_2 = 1087 \Omega$, $R_3 = 32,613 \Omega$, $R_4 = 9944 \Omega$ and $C_1 = C_2 = C_3 = C_4 = 4.88 \times 10^{-10} \text{ F}$. By using these as initial guesses, the values of the components were obtained accurately by running the CNLS program IMPSPEC.BAS developed by one of the authors [22] and being regularly used by us. These values were $R_1 = (0.77 \pm 0.01) \text{ k}\Omega$, $C_1 = (0.38 \pm 0.01) \text{ nF}$, $R_2 = (3.43 \pm 0.02) \text{ k}\Omega$, $C_2 = (0.44 \pm 0.01) \text{ nF}$, $R_3 = (10.87 \pm 0.09) \text{ k}\Omega$, $C_3 = (1.08 \pm 0.06) \text{ nF}$, $R_4 = (15.36 \pm 0.26) \text{ k}\Omega$ and $C_4 = (5.81 \pm 0.09) \text{ nF}$. The M' and M'' values corresponding to the fitted RC's are also shown in **Figure 7(c)**.

Use of different models for impedance spectroscopy of few other ceramics is briefly described now. Analysis of data for SrTiO_3 borosilicate glass ceramics having

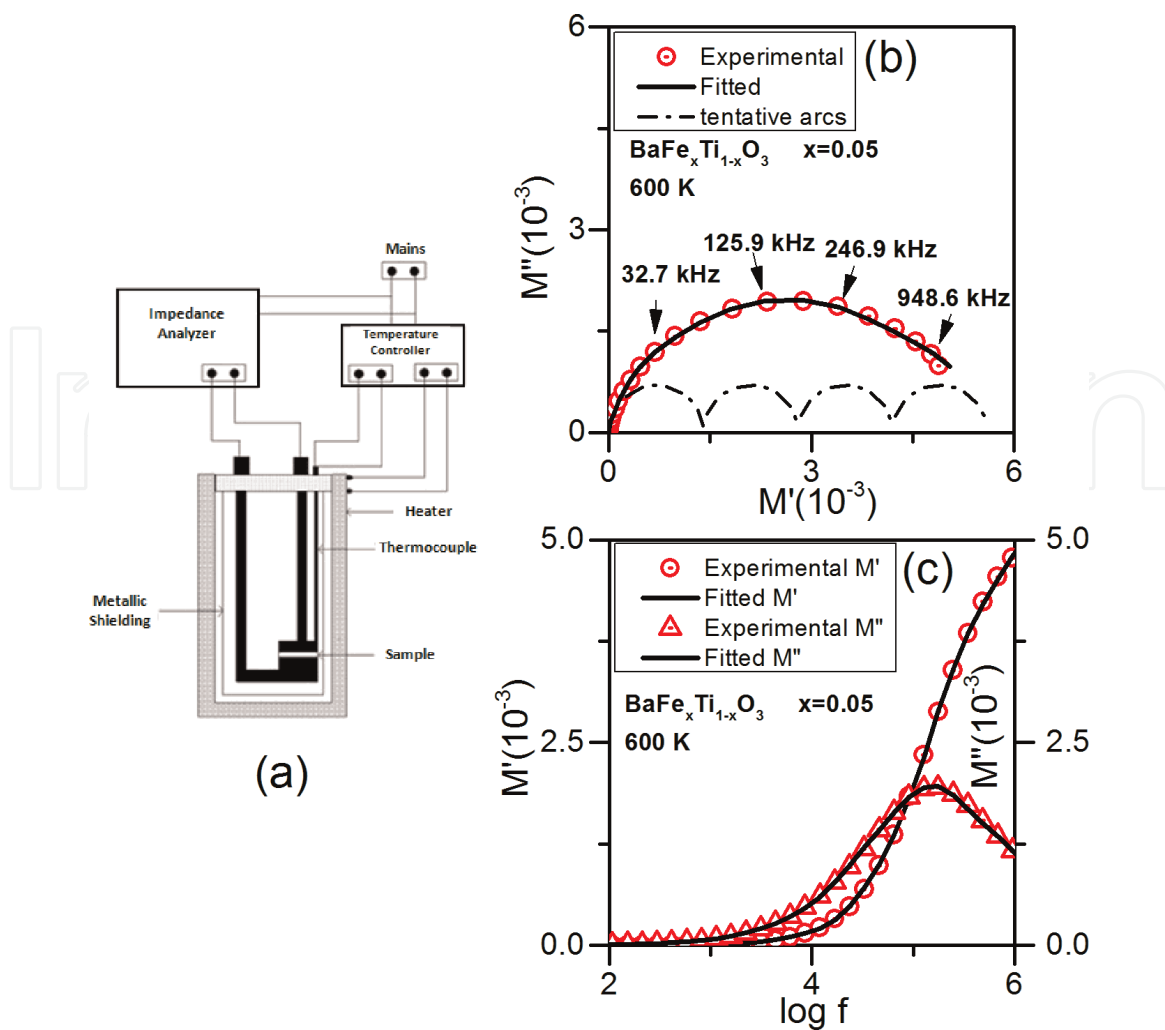


Figure 7.

(a) Experimental Setup for Impedance Measurements. Experimental and fitted values of (b) M'' vs M' for $\text{BaFe}_x\text{Ti}_{1-x}\text{O}_3$ ($x = 0.05$) at 600 K and (c) M' , M'' vs $\log f$ for $\text{BaFe}_x\text{Ti}_{1-x}\text{O}_3$ $x = 0.05$ at 600 K.

steeply rising low-frequency branch in Z'' vs. Z' plots has been done by Pandey et al. [17]. $\text{Ba}_{1-x}\text{La}_x\text{Ti}_{1-x}\text{Co}_x\text{O}_3$ ($x \leq 0.20$) ceramic showed a shifted arc in Z'' vs. Z' plot and was analysed by using equivalent circuit model involving a series resistance [19]. In this system, presence of two PTCR components, one due to grain boundary as usual and the other in grains was observed by impedance spectroscopy. Study of semiconducting BaTiO_3 was carried out by using a model containing series resistance [18]. Ceramic system $\text{Ca}_{1-x}\text{Y}_x\text{Ti}_{1-x}\text{Co}_x\text{O}_3$ could be represented by an equivalent circuit model containing two parallel RC's and a CPE connected in series [21]. Models useful for representing magnetic ceramic are not covered in this paper. A detailed analysis of models involving inductive component L is available in [11] where magnetic ceramic YIG has been studied by using impedance spectroscopy.

While using the impedance spectroscopy, it is important to keep in mind that the observed impedance values are those what the impedance analyser sees at its input points. These values include the contributions from the connecting leads, cables, sample holder and electrodes. It has been found that the electrode-sample contact behaviour changes with the nature of the sample [15]. The sample-electrode contact effects have been studied in detail in [23–35]. A method has been proposed for removing the sample holder contributions [23], which involves doing the complete impedance spectroscopic analysis without the sample, finding an empirical functional relation for the impedance behaviour and then subtracting this from the results obtained with sample placed in the sample holder. Presently available analysers provide with a lead correction step before an actual measurement is done.

For separating out contact contributions, impedance spectroscopic studies by repeating the measurements with changed electrodes have been reported [36]. Measurements by using samples of different thicknesses might also be useful. Various sources of errors in impedance measurements have been discussed in [6].

5. Conclusion

Some equivalent circuit models most useful for impedance spectroscopic studies of electronic ceramics and their simulated immittance behaviour are discussed. In order to facilitate prompt development of equivalent circuit models, few extremely helpful steps have been summarised. A comparison of the experimental plots with simulated ones provides a clue for inclusion of certain lumped components in the model, e.g. a right shift in the Z'' vs. Z' plot indicates presence of series resistance and a shift in M'' vs. M' plot indicates presence of series capacitance in the model. The models are not unique. The most appropriate model may be arrived at by looking at the immittance plots in more than one formalisms (such as Z and M) for all the experimental parameters such as composition, temperature etc, taken together, and considering the possibilities of processes present/dormant, emerging or dominating in the system as some variables such as temperature are altered. The procedure of impedance spectroscopic modelling is illustrated by analysing the impedance data on the ceramic system $\text{BaFe}_x\text{Ti}_{1-x}\text{O}_3$ ($x = 0.05$) containing two phases.

Acknowledgements

The financial support received by one of the authors (SP) from IIT(BHU) in the form of Teaching Assistantship is gratefully acknowledged.

Author details


Shukdev Pandey^{1*}, Devendra Kumar¹, Om Parkash¹ and Lakshman Pandey²

¹ Department of Ceramic Engineering, IIT(BHU), Varanasi, India

² Department of Physics and Electronics, Rani Durgavati University, Jabalpur, India

*Address all correspondence to: spandey.rs.cer12@itbhu.ac.in

IntechOpen

© 2018 The Author(s). Licensee IntechOpen. This chapter is distributed under the terms of the Creative Commons Attribution License (<http://creativecommons.org/licenses/by/3.0>), which permits unrestricted use, distribution, and reproduction in any medium, provided the original work is properly cited. 

References

- [1] Moulson AJ, Herbert JM. Electro-ceramics. 2nd ed. England: John Wiley & Sons Ltd.; 2003
- [2] Buchanan RC. Ceramic Materials for Electronics. 3rd ed. New York: CRC Press; 2004
- [3] Sebastian MT. Dielectric Materials for Wireless Communications. 1st ed. Oxford: Elsevier Ltd; 2008
- [4] Callister WD Jr. Materials Science and Engineering : An Introduction. 7th ed. New York: John Wiley & Sons Inc; 2007
- [5] MacMillan PW. Glass Ceramics. 2nd ed. London: Academic Press; 1979
- [6] Barsoukov E, Macdonald JR. Impedance Spectroscopy Theory, Experiment, and Applications. 2nd ed. New Jersey: John Wiley & Sons; 2005
- [7] Jonscher AK. Dielectric Relaxation in Solids. 1st ed. London: Chelsea Dielectric Press; 1983
- [8] Pandey L, Parkash O, Katare RK, Kumar D. Equivalent circuit models for electronic ceramics. Bulletin of Materials Science. 1995;18:563-576. DOI: 10.1007/BF02744842
- [9] Pandey S, Kumar D, Parkash O, Pandey L. Equivalent circuit models using CPE for impedance spectroscopy of electronic ceramics. Integrated Ferroelectrics. 2017;183:141-162. DOI: 10.1080/10584587.2017.1376984
- [10] Sinclair DC, West AR. Effect of atmosphere on the PTCR properties of BaTiO₃ ceramics. Journal of Materials Science. 1994;29:6061-6068. DOI: 10.1007/BF00354542
- [11] Katare RK, Pandey L, Dwivedi RK, Parkash O, Kumar D. A novel approach based on impedance spectroscopy for measurement of magnetic permeability of ceramics. Indian Journal of Engineering & Materials Sciences. 1999; 6:34-42. <http://nopr.niscair.res.in/handle/123456789/21976>
- [12] Katare RK. Application of Impedance Spectroscopy in the Study of Electronic Ceramics [thesis]. Jabalpur, India: Rani Durgavati University; 1997
- [13] Chaitanya P. Impedance Spectroscopy and RF Pulse Response of Piezoelectric Materials. [Thesis]. Jabalpur, India: Rani Durgavati University; 2009
- [14] Chaitanya P, Shukla A, Pandey L. Determination of equivalent circuit model components of piezoelectric materials by using impedance spectroscopy. Integrated Ferroelectrics. 2014;150:88-95. DOI: 10.1080/10584587.2014.874274
- [15] Chaitanya P, Mishra R, Ahirwal P, Shukla A, Thakur OP, Pandey L, et al. Study of temperature dependence of electrode-glass ceramic interface using impedance spectroscopy. Integrated Ferroelectrics. 2015;159:121-126. DOI: 10.1080/10584587.2015.1033048
- [16] Chaitanya P, Thakur OP, Kumar V, Shukla A, Pandey L. Equivalent circuit model of a PbZr_{0.6}Ti_{0.4}O₃ ceramic using impedance spectroscopy. Journal of Ceramic Processing Research. 2011;12: 247-258
- [17] Pandey L, Katare RK, Parkash O, Kumar D, Thakur OP. Complex impedance analysis of electronic ceramics showing steeply rising impedance pattern at low frequency. Indian Journal of Pure & Applied Physics. 1998;36:228-235
- [18] Maiti HS, Basu RN. Complex plane impedance analysis for semiconducting barium titanate. Materials Research

Bulletin. 1986;**21**:1107-1114. DOI: 10.1016/0025-5408(86)90227-8

[19] Pandey L, Katare RK, Parkash O, Kumar D. Evidence of two ferroelectric PTCR components in valence compensated ceramic system $\text{Ba}_{1-x}\text{La}_x\text{Ti}_{1-x}\text{Co}_x\text{O}_3$. Bulletin of Materials Science. 1997;**20**:933-947. <https://www.ias.ac.in/article/fulltext/boms/020/07/0933-0947>

[20] Kumar V, Thakur OP, Pandey L, Guimaraes AP, Goel A, Parkash O, et al. Modeling of electrical behavior of $\text{La}_{0.7}\text{Ca}_{0.3}\text{MnO}_3$ ceramic using impedance spectroscopy. Modern Physics Letters B. 2005;**19**:697-706. DOI: 10.1142/S0217984905008621

[21] Katare RK, Pandey L, Thakur OP, Parkash O, Kumar D. Equivalent circuit model of $\text{Ca}_{1-x}\text{Y}_x\text{Ti}_{1-x}\text{Co}_x\text{O}_3$ using impedance spectroscopy. Modern Physics Letters B. 2003;**17**:339-346. DOI: 10.1142/S0217984903005238

[22] Pandey L. In: Workshop on Use of Computers in Teaching Physics; Partly Sponsored by ICTP; 3–9 December 1992; Jabalpur, India

[23] Pandey L, Parkash O, Kumar D. On sample holder corrections in the complex impedance analysis of electronic ceramics. Indian Journal of Pure & Applied Physics. 1996;**34**: 28-33

[24] Edwards DD, Hwang JH, Ford SJ, Mason TO. Experimental limitations in impedance spectroscopy: Part V. Apparatus contributions and corrections. Solid State Ionics. 1997;**99**: 85-93. DOI: 10.1016/S0167-2738(97)00206-3

[25] Basu RN, Maiti HS. PTC behaviour of semiconducting BaTiO_3 ceramics. Transactions of the Indian Ceramic Society. 1986;**45**:140-146. DOI: 10.1080/0371750X.1986.10822812

[26] Deguin A, Moretti P, Boyeaux JP. Electrical properties of Nb doped BaTiO_3 crystal with special emphasis on contact influence. Ferroelectrics. 1980; **26**:761-764. DOI: 10.1080/00150198008008166

[27] Serghei A, Tress M, Sangoro JR, Kremer F. Electrode polarization and charge transport at solid interfaces. Physical Review B. 2009;**80**: 184301-184305. DOI: 10.1103/PhysRevB.80.184301

[28] Sato H, Manghna MH, Lienert BR, Weiner A. Effects of sample-electrode interface polarization on the electrical properties of partially molten rock. Journal of Geophysical Research. 1986; **91**:9325-9332. DOI: 10.1029/JB091iB09p09325

[29] Pizzitutti F, Bruni F. Electrode and interfacial polarization in broadband dielectric spectroscopy measurements. Review of Scientific Instruments. 2001; **72**:2502-2504. DOI: 10.1063/1.1364663

[30] Ahmed R, Reifsnider K. Study of influence of electrode geometry on impedance spectroscopy. International Journal of Electrochemical Science. 2011;**6**:1159-1174

[31] Costa MEV, Mantas PQ, Baptista JL. Effect of electrode alterations on the a.c. behaviour of $\text{Li}_2\text{O}-\text{ZnO}$ humidity sensors. Sensors and Actuators B. 1995; **26-27**:312-314. DOI: 10.1016/0925-4005(94)01608-K

[32] Hsieh G, Ford SJ, Mason TO, Pederson LR. Experimental limitations in impedance spectroscopy: Part I—Simulation of reference electrode artifacts in three-point measurements. Solid State Ionics. 1996;**91**:191-201. DOI: 10.1016/S0167-2738(96)83019-0

[33] Hsieh G, Mason TO, Pederson LR. Experimental limitations in impedance spectroscopy: Part II—Electrode artifacts in three-point measurements on Pt/YSZ.

Solid State Ionics. 1996;**91**:203-212. DOI:
10.1016/S0167-2738(96)83020-7

[34] Hsieh G, Mason TO, Garboczi EJ,
Pederson LR. Experimental limitations
in impedance spectroscopy: Part III.
Effect of reference electrode geometry
position. Solid State Ionics. 1997;**96**:
153-172. DOI: 10.1016/S0167-2738(97)
00073-8

[35] Hwang JH, Kirkpatrick KS, Mason
TO, Garboczi EJ. Experimental
limitations in impedance spectroscopy:
Part IV. Electrode contact effects. Solid
State Ionics. 1997;**98**:93-104. DOI:
10.1016/S0167-2738(97)00075-1

[36] Maso N, Beltran H, Cordoncillo E,
Escribano P, West AR. Electrical
properties of Fe-doped BaTiO₃. Journal
of Materials Chemistry. 2006;**16**:
1626-1633. DOI: 10.1039/B515834F